ARTICLE

Control of Self-Assembly of Lithographically Patternable Block Copolymer Films

Joan K. Bosworth,[†] Marvin Y. Paik,[†] Ricardo Ruiz,[‡,⊥] Evan L. Schwartz,[†] Jenny Q. Huang,[†] Albert W. Ko,[†] Detlef-M. Smilgies,[§] Charles T. Black,[‡,||] and Christopher K. Ober[†,*]

[†]Department of Materials Science and Engineering, Bard Hall, Cornell University, Ithaca, New York 14853, [‡]IBM T. J. Watson Research Center, Yorktown Heights, New York 10598, and [§]Cornell High Energy Synchrotron Source, Wilson Laboratory, Cornell University, Ithaca, New York 14853. [⊥]Present address: Hitachi Global Storage Technologies, San Jose, CA 95135. [||]Present address: Center for Functional Nanomaterials, Brookhaven National Laboratory, Upton, New York 11973.

ABSTRACT Poly(α-methylstyrene)-*block*-poly(4-hydroxystyrene) acts as both a lithographic deep UV photoresist and a self-assembling material, making it ideal for patterning simultaneously by both top-down and bottom-up fabrication methods. Solvent vapor annealing improves the quality of the self-assembled patterns in this material without compromising its ability to function as a photoresist. The choice of solvent used for annealing allows for control of the self-assembled pattern morphology. Annealing in a nonselective solvent (tetrahydrofuran) results in parallel orientation of cylindrical domains, while a selective solvent (acetone) leads to formation of a trapped spherical morphology. Finally, we have self-assembled both cylindrical and spherical phases within lithographically patterned features, demonstrating the ability to precisely control ordering. Observing the time evolution of switching from cylindrical to spherical morphology within these features provides clues to the mechanism of ordering by selective solvent.

KEYWORDS: self-assembly · block copolymer · photoresist · solvent annealing · graphoepitaxy · PαMS-*b*-PHOST

*Address correspondence to cober@ccmr.cornell.edu.

Received for review March 12, 2008 and accepted June 04, 2008.

Published online July 22, 2008.
10.1021/nn8001505 CCC: $40.75

© 2008 American Chemical Society

Patterning the nanometer-scale dimensions of microelectronic integrated circuit (IC) elements continues to be a major technological barrier to realizing performance improvements.[1] One proposed pathway to achieving patterning objectives for future IC generations involves designing increased functionality into the polymeric resist patterning materials. For example, a single resist material that is patternable by both conventional deep UV lithography (*i.e.*, a top-down method) as well as self-assembly techniques (*i.e.*, bottom-up methods) provides a vehicle for efficiently implementing both approaches within the technology infrastructure of advanced lithographic patterning.

The diblock copolymer poly(α-methylstyrene)-*block*-poly(4-hydroxystyrene) (PαMS-*b*-PHOST) is a distinctive material because it is patternable by both deep UV lithography and self-assembly techniques.[2,3] This feature, along with the selective removal of the PαMS minor phase, allows for very precise location of the self-assembled block copolymer pattern that can be used for further patterning applications, especially when coupled with the selective removal of the PαMS minor phase. However, controlling the microphase separation, demonstrated in this work, is key for device applications. PαMS-*b*-PHOST with overall molecular weight of 21 kg/mol (M_w/M_n 1.10) and mass fraction of PαMS 33% forms disordered, though perpendicularly oriented, cylindrical domains upon spin casting from a solvent of propylene glycol methyl ether acetate (PGMEA) (Figure 1a), regardless of substrate, and for a wide range of film thicknesses. The observed behavior is consistent with reports that a solvent evaporation gradient across the polymer film can promote a perpendicular domain orientation with little hexagonal ordering.[4] For PαMS-*b*-PHOST, it is not possible to improve the quality of the self-assembly process *via* a thermal treatment due to the low ceiling temperature[5] and corresponding low decomposition temperature of PαMS, though it is this behavior that allows the selective removal of the PαMS block. We observe thermal degradation of PαMS at a temperature of 150 °C, while we measure the PHOST glass transition temperature of 180−190 °C by differential scanning calorimetry.

Alternatively, solvent annealing has been shown to improve the spatial coherence of patterns in other polymer systems.[6−10] This occurs because the solvent imparts increased polymer chain mobility by acting as a plasticizer, thus effectively lowering the glass transition temperature, T_g, and increasing the mobility of the polymer chains.[11] Additionally, the

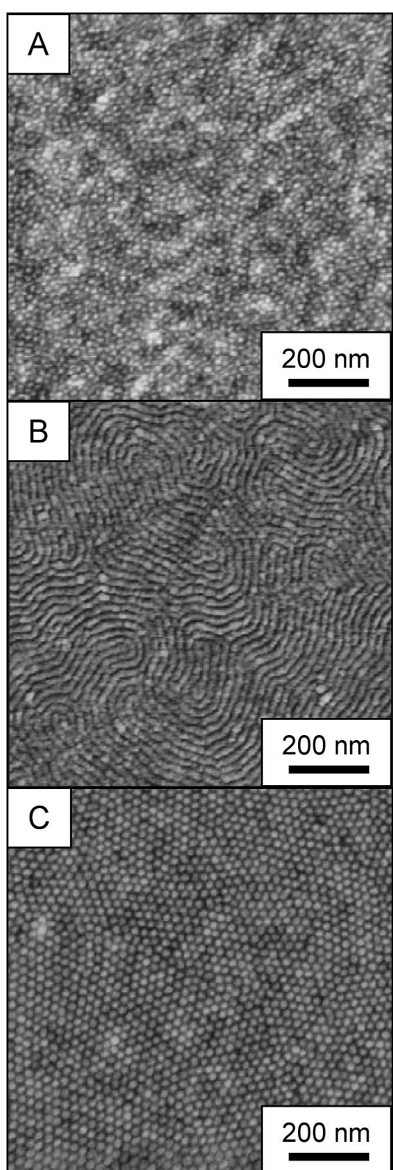

Figure 1. Atomic force height micrographs of PαMS-*b*-PHOST films with 16 nm thickness. (a) As cast, perpendicularly oriented cylindrical phase. (b) Parallel-oriented cylinders after annealing in THF. (c) Hexagonally packed dot pattern after acetone anneal. In AFM, PαMS appears as the lighter color.

selectivity of the solvent for the two block allows further control of the morphology formed by the polymer upon swelling and locked in upon rapid evaporation.

Further control of morphology location is necessary for patterning applications. Additional techniques can be used in conjunction with polymer mobility techniques (either thermal or solvent annealing) in order to gain further control of morphology, including electric fields,[12−14] shear,[15−17] chemically patterned substrates,[18,19] and graphoepitaxy.[8,20−23] Graphoepitaxy, or self-aligned self-assembly, is particularly interesting because the polymer morphology can subdivide a much larger feature created by traditional photolithographic techniques.

RESULTS AND DISCUSSION

Solvent Swelling Imparts Mobility and Morphology Control. Because of the difficulties associated with thermal treatments, we have instead used solvent vapor annealing to promote uniform self-assembly of PαMS-*b*-PHOST thin films. We observe parallel cylinder domain orientation when polymer chains gain mobility due to swelling in tetrahydrofuran (THF) (Figure 1b), a good solvent for both polymer blocks.[24] In this case, preferential surface wetting by the PHOST block drives parallel domain orientation. We measure the cylinder center-to-center distance of 22 nm by atomic force microscopy (AFM) and film thickness of 16 nm by ellipsometry and 14 nm by profilometry; the same annealing behavior is observed for thicker films (127 nm by profilometry), as well. In the case of PαMS-*b*-PHOST annealed in THF, sufficient contrast for AFM imaging is achieved by a brief exposure to a gentle oxygen plasma to remove the top few nanometers of the film; no treatment is necessary for as-spun and acetone-annealed films.[25] The presence of a top uniform polymer surface layer indicates a preferential block affinity for the polymer−air interface.

A unique advantage of solvent annealing over thermal treatments is the ability to control block copolymer domain morphology through choice of solvent. Annealing in acetone causes the diblock copolymer film to assemble into a hexagonal array of dots (Figure 1c), with improved order as compared to the as-deposited films (Figure 1a). These top-down images are consistent with either perpendicularly oriented cylindrical domains or spherical morphology. Acetone is not a good solvent for PαMS,[24] though we have found it to be a good solvent for the PHOST homopolymer. Thus, we expect acetone to preferentially swell the PHOST block, inducing an order−order transition from cylindrical to spherical morphology in the swollen state, which may be kinetically trapped in the dried state. It is difficult to distinguish a perpendicular cylinder morphology from a spherical phase in film thicknesses equal to or less than a single morphology period. Thicker films (127 nm, measured by profilometry) that have been annealed in acetone also display the same ordered arrays of dots in AFM images of the top surface (Figure 2a).

Acetone Anneal Yields Spherical Morphology. Grazing incidence small-angle X-ray scattering (GISAXS) is a probe well-suited for studying the polymer film interior, used here to determine the interior structure of the dried films after annealing in acetone. The GISAXS image in Figure 2b prominently features a sharp Bragg reflection at nonzero wavevector (parallel component $q_{\|} = 0.0279$ Å^{-1}, perpendicular component $q_z = 0.0595$ Å^{-1}) indicative of three-dimensional organization inside the film. Additionally, there are two peaks in the Yoneda band between the critical angles of the substrate and film, whose $q_{\|}$ values of 0.0327 and 0.0455 Å^{-1} differ from the first reflection. Moreover, the image does not show the familiar diffuse Bragg rods characteristic of

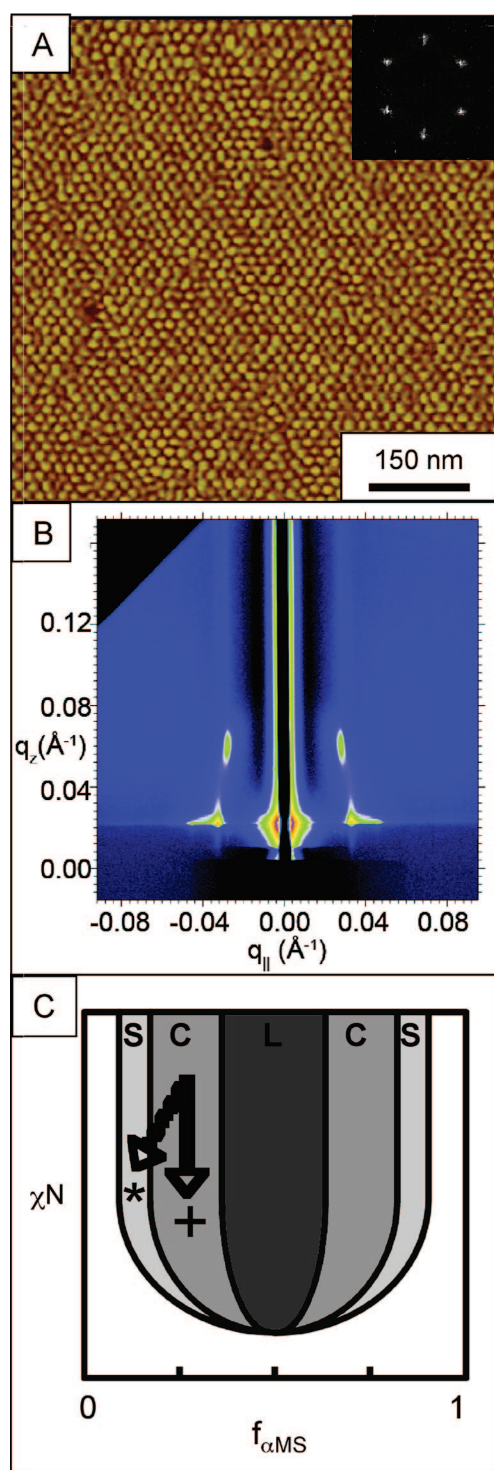

Figure 2. (a) AFM phase image of thick PαMS-*b*-PHOST film after annealing in acetone vapor. (b) Corresponding GISAXS image, demonstrating a face-centered orthorhombic (FCO) lattice in the dried state. (c) Schematic phase diagram of χN *versus* $f_{\alpha MS}$. The solid arrow represents behavior of THF solvent annealing, while the dotted arrow represents acetone annealing. The effective χN parameter of the blocks is modified by the solvent uptake during swelling in both solvents (vertical component of lines). Acetone annealing swells the PHOST block selectively and thus also shifts the volume ratio $f_{\alpha MS}$, while THF swells both blocks equally.

perpendicular cylinders,[2,3,26,27] and thus we conclude that the film does not possess that morphology.

We expect a (110) oriented body-centered cubic (BCC), rather than a hexagonally close-packed lattice of spheres, in the swollen state of these multilayer polymer film samples comprising several layers of spheres.[28] Our data indicate that the rapid evaporation of the solvent from the film upon removal from the chamber kinetically traps the spherical morphology, and the deswelling affects the spacing of the spheres in the direction perpendicular to the surface, resulting in a distorted BCC lattice.

A BCC lattice with the (110) plane parallel to the substrate was used in a first attempt to model the observed peak positions. From the lateral peaks in the Yoneda band,we calculate a lattice parameter of 27.5 nm, which corresponds to a spacing of spheres on the top (surface) plane of 24 nm, in reasonable accordance with AFM measurements. However, the observed q_z value of the 3D Bragg reflection suggests film shrinkage in the *z*-direction. Redefining the (110) oriented BCC lattice to a face-centered orthorhombic (FCO) surface lattice allows modeling of the distorted system, while maintaining the highest possible lattice symmetry. The resulting theoretical peak positions agree well with the GISAXS measurements—clear evidence that the film transitioned to a BCC spherical morphology in the swollen state, which was then kinetically trapped and deformed in the vertical direction to an FCO spherical morphology upon drying. In the dried state, the FCO lattice constant perpendicular to the substrate is found to be 16.5 nm, indicating that it has been reduced to 42% of the original value (38.9 nm) in the BCC phase of the swollen film. Further explanation of the analysis of these data may be found in the Supporting Information.

The effects of solvent annealing can be visualized in a χN *versus* $f_{P\alpha MS}$ phase diagram, where χ is the Flory−Huggins interaction parameter, N is the degree of polymerization, and $f_{P\alpha MS}$ is the volume fraction of PαMS in the block copolymer (Figure 2c).[9,10] A good solvent for both copolymer blocks (such as THF) is uniformly incorporated by the polymer film and imparts chain mobility by acting as a plasticizer. Such behavior is comparable to a downward vertical shift in χN as $f_{P\alpha MS}$ remains constant. Acetone annealing involves the additional variable of preferential solubility PHOST (over PαMS) in the solvent. An affinity of the solvent for one block changes the volume ratio of the two copolymer blocks comprising the film, such that swelling in a selective solvent changes not just the vertical position in the χN *versus* $f_{P\alpha MS}$ phase diagram but the horizontal position, as well. In this case, the majority component (PHOST) swells more, causing an order−order transition from cylindrical to spherical morphology as the increased PHOST volume changes the diblock copolymer volume fraction of the swollen state so that it assumes the BCC-packed structure. This state remains trapped in the spherical morphology upon rapid drying, though it changes to an FCO lattice when the film

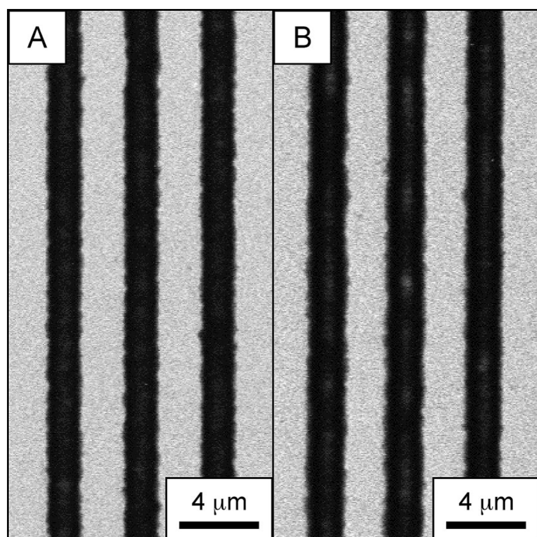

Figure 3. Scanning electron micrograph of photolithographic patterns of PαMS-*b*-PHOST. Films containing TPST photoacid generator and TMMGU cross-linker were exposed (a) as-spun, and (b) after THF solvent annealing. Dark regions are lines of cross-linked polymer left behind after post-exposure bake and development in solvent.

shrinks. Previous experiments on other block copolymer systems have reported the collapse of spherical morphology to a perpendicularly oriented cylindrical phase upon evaporation of a selective solvent[8–10] in contrast to our observations of PαMS-*b*-PHOST *via* GISAXS. This unidirectional contraction of a BCC lattice into an FCO lattice has been observed elsewhere in the case of a Pluronics surfactant upon evaporation of water vapor.[29]

Effect of Solvent on Photoresist Behavior. Thephotoresist properties of PαMS-*b*-PHOST do not alter or interfere with the self-assembly of PαMS-*b*-PHOST polymer films in solvent vapor. The photoacid generator triphenylsulfonium trifluoromethanesulfonate (TPST) and the cross-linker 1,3,4,6-tetrakis(methoxymethyl)glycoluril (TMMGU), in quantities 5% w/w or less, are both necessary for the PαMS-*b*-PHOST to function as a resist.[2] These small quantities have no discernible affect on ordering *via* solvent annealing, as long as the film is not exposed to UV light during the assembly process. Furthermore, the solvent-vapor-assisted self-assembly process does not affect PαMS-*b*-PHOST performance as a UV photoresist when tested in the thicker films. Solvent-annealed films (Figure 3b) containing small amounts of TPST and TMMGU (less than 5% w/w, relative to the polymer) show virtually identical cross-linking behavior to films not exposed to solvent vapor (Figure 3a). The photopatterns were exposed in both as-spun and THF-annealed PαMS-*b*-PHOST films using 248 nm light, a post exposure bake of 115 °C for 60 s (insufficient time for significant PαMS damage), and mixed solvent development with cyclohexanone and isopropanol (1:2 v/v), and the pattern resolution is nearly identical. PαMS-*b*-PHOST films annealed in acetone (not shown) have similar lithographic resolution. This indicates that the photoacid generator and cross-linker do not selectively partition into the PαMS phase in either of the solvent-annealed films, just as it does not in the as-spun films.

Graphoepitaxy. High-resolution lithography applications of self-assembled diblock copolymer films would ultimately require both polymer domain registration and ordering, and we have demonstrated registration of PαMS-*b*-PHOST films to topographic features by solvent annealing. For our experiments, we prepared 30 nm deep topographic features in silicon dioxide (SiO_2) using conventional deep UV lithography and plasma etching techniques.[30] We pretreat the patterned SiO_2 substrates with a PS brush prior to PαMS-*b*-PHOST deposition in order to achieve preferential wetting by the PαMS minority block,[31,32] as the minority block must preferentially wet the substrate in order to avoid pinning effects.[33] The same solution and spin speed that formed 16 nm thick films on flat substrates were used here. We observe registration of parallel-oriented cylinder domains upon annealing in THF (Figure 4a), while films deposited on untreated silicon oxide do not self-align to the patterned sub-

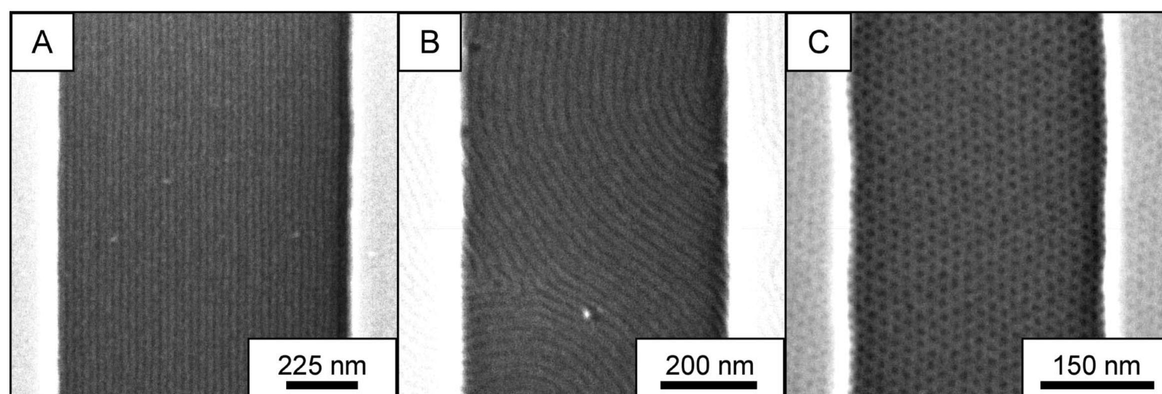

Figure 4. Self-aligned PαMS-*b*-PHOST patterns on lithographically patterned substrates. (a) On PS brush-treated substrates, annealing in THF leads to self-aligned parallel cylinder domains. (b) On SiO_2 substrates without PS brush treatment, annealing in THF does not lead to pattern registration. (c) On SiO_2 substrates without PS brush treatment, annealing in acetone leads to aligned hexagonal dot pattern. In SEM images, darker regions are the PαMS phase.

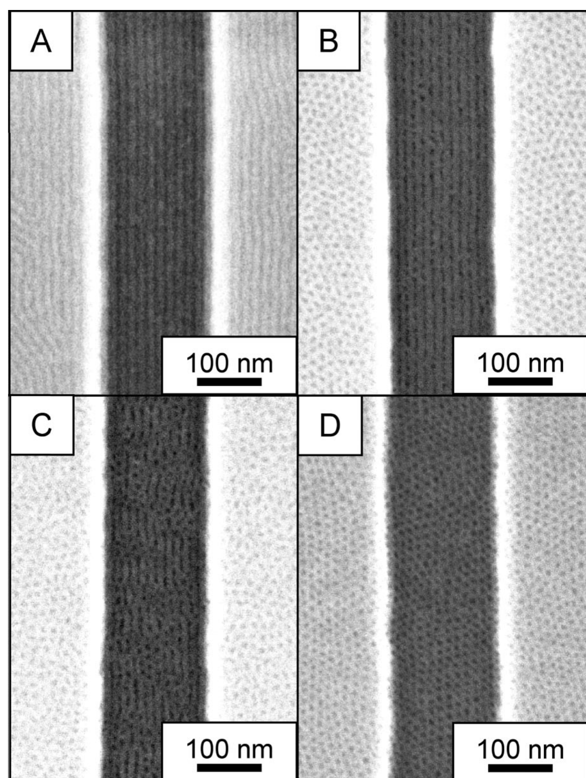

Figure 5. Time evolution of acetone anneal of aligned cylinder pattern on PS-treated substrate: (a) prior to acetone anneal; (b) 3 h acetone anneal; (c) 3.5 h acetone anneal; (d) 5 h acetone anneal.

strate upon THF annealing (Figure 4b). Sufficient contrast for SEM imaging is achieved by partial development of PαMS for SEM imaging; in the case of THF-annealed films, films are briefly exposed to a gentle oxygen plasma,[25] while acetone-annealed films need only to be heated briefly. Cross-sectional SEM revealed film thicknesses of 20 nm within trenches, consistent with a single-morphology thickness. We have achieved defect-free domain alignment of parallel cylinders with 23 nm pitch across trench widths of 840 nm. As the figure shows, the 37 cylindrical domains run distances of over 2 μm without defects.

Solvent annealing PαMS-*b*-PHOST in acetone rather than THF results in aligned hexagonal arrays of dots (Figure 4c). We observe this alignment regardless of substrate treatment, that is, for both native SiO_2 (PHOST preferential surface) and for PS-treated (PαMS preferential) substrates. Figure 4c shows registration of self-assembled patterns to a lithographically patterned (and untreated) SiO_2 trench after acetone annealing, and we have observed similar results for patterned substrates treated with PS brushes. We measure the sphere center-to-center spacing to be 23 nm *via* SEM.

Sequential annealing of aligned PαMS-*b*-PHOST films first in nonpreferential (THF) and then preferential (acetone) solvents allows us to switch from parallel cylinder to spherical morphology, a useful experimental lever for observing the process by which the transition takes place. We have observed by SEM the time evolution of the order−order transition to spherical morphology by acetone annealing an aligned film with parallel cylinder orientation. The initial sample contains oriented parallel cylinder domains spanning a 175 nm wide trench treated with a PS brush (Figure 5a). At intermediate anneal times during the transition, we observe mixed morphology of lines and dots, further supporting that an order−order transition from, in this case, parallel cylindrical to spherical morphology occurs in the swollen film. After 3 h of acetone annealing, independent spheres have begun to form within the trench-aligned pattern (Figure 5b). Note that, in the thinner film areas outside the lithographic trench, complete morphology changes are already completed. After 3.5 h of annealing, patches of spheres disrupt the parallel cylinders (Figure 5c), and after 5 h of annealing, we observe complete hexagonal packing of spheres within the trench region (Figure 5d).

CONCLUSIONS

We have demonstrated for the first time control of self-assembly in registration with predefined structures and with choice of morphology in PαMS-*b*-PHOST diblock copolymer films, a material well-suited to applications because of its patternability by both lithographic and self-assembly approaches. The control provided by reversible solvent annealing processes allows us a window to understanding the fundamental mechanisms of morphology change—in this case, a transition from cylindrical to a trapped spherical phase. The demonstration of development of long-range ordering and control of morphology by solvent annealing in combination with the precise orientation of grains *via* graphoepitaxy are the critical steps needed for application to device fabrication.

METHODS

Synthesis. Poly(α-methylstyrene)-*block*-poly(*tert*-butoxystyrene), PαMS-*b*-PtBuOS, was synthesized *via* sequential anionic polymerization and subsequently deprotected to form PαMS-*b*-PHOST, as described elsewhere.[2] GPC indicates a total number average molecular weight of PαMS-*b*-PtBuOS of 28 kg/mol, 25% by mass PαMS, and with M_w/M_n 1.10. Thus, deprotected PαMS-*b*-PHOST has M_n of 21 kg/mol, 33% PαMS. Complete deprotection was confirmed by FTIR. Polystyrene for surface treatment was synthesized *via* nitroxide-mediated controlled free radical polymerization using TEMPO (2,2,6,6-tetramethylpiperidine 1-oxyl, Aldrich) and benzoyl peroxide (Aldrich) under nitrogen without subsequent removal of the nitroxide end group.[34] The resulting polymer samples have M_n 12.7 kg/mol and M_w/M_n 1.30 according to GPC.

Film Preparation. Solutions of 1 and 5% (w/v) PαMS-*b*-PHOST in PGMEA (Aldrich) were spin-coated onto silicon wafers with na-

tive oxide or onto silicon oxide substrates with 30 nm deep patterns prepared by lithography and etching techniques. Brush treatment consists of a 1% (w/v) solution of polystyrene spin-coated and baked at 195 °C for 2.5 h. Immediately before spin coating with PαMS-*b*-PHOST, excess PS was removed by rinsing with toluene. Solvent vapor treatment with THF or acetone was carried out in a closed jar containing a solvent reservoir. Times for solvent annealing leading to the most ordered films were determined for each solvent and for both thick and thin film thicknesses. Films annealed in THF require partial development for both AFM and SEM imaging; this is acheved by treatment with an oxygen plasma etch, for 9 s at 50 W, 100 mTorr, and 30 sccm oxygen using a PlasmaTherm 72 reactive ion etcher. For imaging as-spun and acetone-annealed films by SEM, partial removal of the PαMS block is achieved by heating in a vacuum oven at 165 °C for 30 min and is sufficient, though the brief oxygen plasma etch is also sufficient; for these films, no special treatment is required for AFM imaging.

The photoacid generator TPST (Aldrich) and the cross-linker TMMGU ("Powderlink 1174," Cytec Industries) were added to the 5% polymer solution in amounts of 5% or less (w/w) relative to the polymer. Films were spin-coated and solvent-annealed, and exposures were made through a quartz mask using a Hybrid Technology Group system III-HR contact mask aligner with deep UV exposure.

Characterization. GPC of THF solutions of polymers (1 mg/mL) was carried out using four Waters Styragel HT columns operating at 40 °C and Waters 490 ultraviolet (254 nm wavelength) and Waters 410 refractive index detectors. Scanning electron microscopy is performed on a LEO 1550 FE-SEM, and atomic force microscopy is performed on a Veeco Dimension 3100. Differential scanning calorimetry was performed on a TA Instruments Q1000. Ellipsometry was performed on a Woollam M-2000, and profilometry was performed on scored films using a Tencor P-10 Surface Profiler. The grazing incidence small-angle X-ray scattering (GISAXS) image in this paper was taken at the G1 line at the Cornell High Energy Synchrotron Source (CHESS). Additional GISAXS has been performed at the D1 beamline at CHESS and at beamline 8-ID-E of the Advanced Photon Source.

Acknowledgment. This work was supported by the National Science Foundation Materials World Network (award DMR 0602821) and the NSF NIRT (award CTS 0304159), and the Semiconductor Research Consortium, and J.K.B. was supported by fellowships from Motorola and IBM. The authors would also like to thank P. Busch, Cornell, and X. Li, Advanced Photon Source, for their help. This work was performed using facilities at the Cornell High Energy Synchrotron Source (CHESS), the Cornell Center for Materials Research (CCMR), and The Cornell NanoScale Facility (CNF). CHESS is supported by the NSF and the National Institutes of Health/National Institute of General Medical Sciences under NSF award DMR-0225180. CCMR is supported by NSF award DMR 0520404, part of the NSF MRSEC Program. CNF, a member of the National Nanotechnology Infrastructure Network, is supported by NSF award ECS-0335765.

Supporting Information Available: Detailed analysis of GISAXS data found in Figure 2b. This material is available free of charge *via* the Internet at http://pubs.acs.org.

REFERENCES AND NOTES

1. The International Technology Roadmap for Semiconductors, 2007 Edition; http://www.itrs.net/Links/2007ITRS/Home2007.htm (May 17, 2008).
2. Li, M.; Douki, K.; Goto, K.; Li, X.; Coenjarts, C.; Smilgies, D. M.; Ober, C. K. Spatially Controlled Fabrication of Nanoporous Block Copolymers. *Chem. Mater.* **2004**, *16*, 3800–3808.
3. Du, P.; Li, M.; Douki, K.; Li, X.; Garcia, C. B. W.; Jain, A.; Wiesner, U.; Ober, C. K. Additive-Driven Phase-Selective Chemistry in Block Copolymer Thin Films: The Convergence of Top-Down and Bottom-Up Approaches. *Adv. Mater.* **2004**, *16*, 953–957.
4. Lin, Z.; Kim, D. H.; Wu, X.; Boosahda, L.; Stone, D.; LaRose, L.; Russell, T. P. A Rapid Route to Arrays of Nanostructures in Thin Films. *Adv. Mater.* **2002**, *14*, 1373–1376.
5. Ivin, K. J.; Leonard, J. The Effect of Polymer Concentration on the Equilibrium Monomer Concentration for the Anionic Polymerization of α-Methylstyrene in Tetrahydrofuran. *Eur. Polym. J.* **1970**, *6*, 331–341.
6. Fukunaga, K.; Elbs, H.; Magerle, R.; Krausch, G. Large-Scale Alignment of ABC Block Copolymer Microdomains *via* Solvent Vapor Treatment. *Macromolecules* **2000**, *33*, 947–953.
7. Cavicchi, K. A.; Berthiaume, K. J.; Russell, T. P. Solvent Annealing Thin Films of Poly(isoprene-*b*-lactide). *Polymer* **2005**, *46*, 11635–11639.
8. Kim, S. H.; Misner, M. J.; Xu, T.; Kimura, M.; Russell, T. P. Highly Oriented and Ordered Arrays From Block Copolymers *via* Solvent Evaporation. *Adv. Mater.* **2004**, *16*, 226–231.
9. Sidorenko, A.; Tokarev, I.; Minko, S.; Stamm, M. Ordered Reactive Nanomembranes/Nanotemplates from Thin Films of Block Copolymer Supramolecular Assembly. *J. Am. Chem. Soc.* **2003**, *125*, 12211–12216.
10. Tokarev, I.; Krenek, R.; Burkov, Y.; Schmeisser, D.; Sidorenko, A.; Minko, S.; Stamm, M. Microphase Separation in Thin Films of Poly(styrene-*block*-4-vinylpyridine) Copolymer-2-(4′-Hydroxybenzeneazo)Benzoic Acid Assembly. *Macromolecules* **2005**, *38*, 507–516.
11. Mori, K.; Okawara, A.; Hashimoto, T. Order−Disorder Fluctuations of Polystyrene-*block*-polyisoprene. I. Thermal Concentration Fluctuations in Single-Phase Melts and Solutions and Determination of χ as a Function of Molecular Weight and Composition. *J. Chem. Phys.* **1996**, *104*, 7765–7777.
12. Amundson, K.; Helfand, E.; Quan, X.; Hudson, S. D.; Smith, S. D. Alignment of Lamellar Block Copolymer Microstructures in an Electric field. 2. Mechanisms of Alignment. *Macromolecules* **1994**, *27*, 6559–6570.
13. Xu, T.; Zhu, Y.; Gido, S. P.; Russell, T. P. Electric Field Alignment of Symmetric Diblock Copolymer Thin Films. *Macromolecules* **2004**, *37*, 2625–2629.
14. Boeker, A.; Elbs, H.; Haensel, H.; Knoll, A.; Ludwigs, S.; Zettl, H.; Zvelindovsky, A. V.; Sevink, G. J. A.; Urban, V.; Abetz, V. Electric Field Induced Aligment of Concentrated Block Copolymer Solutions. *Macromolecules* **2003**, *36*, 8078–8087.
15. Chen, Z.-R.; Kornfield, J. A.; Smith, S. D.; Grothaus, J. T.; Satkowski, M. M. Pathways to Macroscale Order in Nanostructured Block Copolymers. *Science* **1997**, *277*, 1248–1253.
16. Angelescu, D. E.; Waller, J. H.; Adamson, D. H.; Deshpande, P.; Chou, S. Y.; Register, R. A.; Chaikin, P. M. Macroscopic Orientation of Block Copolymer Cylinders in Single-Layer Films by Shearing. *Adv. Mater.* **2004**, *16*, 1736–1740.
17. Hamley, I. W. The Effect of Shear on Ordered Block Copolymer Solutions. *Curr. Opin. Colloid Interface Sci.* **2000**, *5*, 341–349.
18. Heier, J.; Genzer, J.; Kramer, E. J.; Bates, F. S.; Walheim, S.; Krausch, G. Transfer of a Chemical Substrate Pattern into an Island Forming Diblock Copolymer Film. *J. Chem. Phys.* **1999**, *111*, 11101–11110.
19. Edwards, E. W.; Montague, M. F.; Solak, H. H.; Hawker, C. J.; Nealey, P. F. Precise Control over Molecular Dimensions of Block Copolymer Domains Using the Interfacial Energy of Chemically Nanopatterned Substrates. *Adv. Mater.* **2004**, *16*, 1315–1319.
20. Segalman, R. A.; Yokoyama, H.; Kramer, E. J. Graphoepitaxy of Spherical Domain Block Copolymer Films. *Adv. Mater.* **2001**, *13*, 1152–1155.
21. Cheng, J. Y.; Ross, C. A.; Smith, H. I.; Thomas, E. L. Templated Self-Assembly of Block Copolymers: Top-Down Helps Bottom-Up. *Adv. Mater.* **2006**, *18*, 2505–2521.
22. Black, C. T. Self-Aligned Self Assembly of Multi-Nanowire Silicon Field Effect Transistors. *Appl. Phys. Lett.* **2005**, *87*, 163116.

23. Sundrani, D.; Darling, S. B.; Sibener, S. J. Heirarchical Assembly and Compliance of Aligned Nanoscale Polymer Cylinders in Confinement. *Langmuir* **2004**, *20*, 5091–5099.
24. Bloch, D. R. Solvents and Non Solvents for Polymers. In *Polymer Handbook*, 4th ed.; Brandrup, J., Immergut, E. H., Grulke, E. A., Eds.; John Wiley & Sons: New York, 2003; Section*7*, p 507.
25. Asakawa, K.; Hiraoka, T. Nanopatterning With Microdomains of Block Copolymers Using Reactive-Ion Etching Selectivity. *Jpn. J. Appl. Phys.* **2002**, *41*, 6112–6118.
26. Lin, Y.; Boeker, A.; He, J.; Sill, K.; Xiang, H.; Abetz, C.; Li, X.; Wang, J.; Emrick, T.; Long, S. Self-Directed Self-Assembly of Nanoparticle/Copolymer Mixtures. *Nature* **2005**, *434*, 55–59.
27. Kim, S. H.; Misner, M. J.; Yang, L.; Gang, O.; Ocko, B. M.; Russell, T. P. Salt Complexation in Block Copolymer Thin Films. *Macromolecules* **2006**, *39*, 8473.
28. Stein, G. A.; Kramer, E. J.; Li, X.; Wang, J. Layering Transitions in Thin Films of Spherical-Domain Block Copolymers. *Macromolecules* **2007**, *40*, 2453–2460.
29. Urade, V. N.; Hillhouse, H. W. Synthesis of Thermally Stable Highly Ordered Nanoporous Tin Oxide Thin Films With a 3D Face-Centered Orthorhombic Nanostruture. *J. Phys. Chem. B* **2005**, *109*, 10538–10541.
30. Black, C. T.; Bezencenet, O. Nanometer-Scale Pattern Registration and Alignment by Directed Diblock Copolymer Self-Assembly. *IEEE Trans. Nanotechnol.* **2004**, *3*, 412–415.
31. Mansky, P.; Russell, T. P.; Hawker, C. J.; Pitsikalis, M.; Mays, J. Ordered Diblock Copolymer Films on Random Copolymer Brushes. *Macromolecules* **1997**, *30*, 6810–6813.
32. Mansky, P.; Russell, T. P.; Hawker, C. J.; Mays, J.; Cook, D. C.; Satija, S. K. Interfacial Segregation in Disordered Block Copolymers: Effect of Tunable Surface Potentials. *Phys. Rev. Lett.* **1997**, *79*, 237–240.
33. Harrison, C.; Chaikin, P. M.; Huse, D. A.; Register, R. A.; Adamson, D. H.; Daniel, A.; Huang, E.; Mansky, P.; Russell, T. P.; Hawker, C. J. Reducing Substrate Pinning of a Block Copolymer Microdomains with a Buffer Layer of Polymer Brushes. *Macromolecules* **2000**, *33*, 857–865.
34. Hawker, C. J. Molecular Weight Control by a "Living" Free-Radical Polymerization Process. *J. Am. Chem. Soc.* **1994**, *116*, 11185–11186.